Design of an optimized porous disk to match wake properties of a floating wind turbine

Journal of Physics: Conference Series **3224** (2026) 082016 doi:10.1088/1742-6596/3224/8/082016

Design of an optimized porous disk to match wake properties of a floating wind turbine

Giulia Pomaranzi[1], Federico Taruffi[2], Axelle Viré[2] and Alberto Zasso[1]

[1]Department of Mechanical Engineering, Politecnico di Milano, Milano, Italy
[2]Faculty of Aerospace Engineering, Delft University of Technology, Delft, the Netherlands

E-mail: giulia.pomaranzi@polimi.it

Abstract. Experimental studies of floating offshore wind farms are constrained by scaling limitations that make the use of bladed rotors impractical at the wind farm scale. Porous disks mounted on moving platforms therefore represent a viable alternative, provided that their design reliably reproduces turbine wake characteristics. This work proposes a rational design methodology for porous disks based on a Darcy–Forchheimer porous media formulation within a computational fluid dynamics framework, in which resistance coefficients are directly linked to the disk solidity distribution. Three disk designs with different radial solidity distributions, all matching the thrust coefficient of a reference three-bladed rotor, are investigated under static and imposed-motion conditions. The results show that the solidity distribution mainly affects the near- and mid-wake structure, while its influence diminishes downstream. A non-uniform solidity distribution based on blade loading provides the closest agreement with experimental wake data. Under imposed motions, the optimized disk captures very well the mean wake deficit, with a slightly slower recovery than the bladed rotor limited to the surge case. The proposed methodology provides practical guidance for the physical realization of porous disks in floating wind farm experiments.

1. Introduction

Offshore wind farms are expected to play a major role in expanding installed capacity by providing access to vast wind resources [1]. The deployment of floating offshore wind turbines enables the exploitation of deep-water sites but also introduces additional challenges related to wake interactions and platform-induced unsteadiness at the wind farm scale.

Investigating wake interactions in floating wind farms through experimental testing with scaled rotors is subject to fundamental scaling limitations. While wind tunnel testing with bladed rotors is feasible for isolated turbines, extending such experiments to wind farm scales rapidly becomes unfeasible: at the required geometric scaling, bladed rotors become prohibitively small, making impossible to rely on bladed rotor models for experimental studies of floating wind farms, requiring instead simplified turbine representations.

In this context, porous disks mounted on moving platforms could offer a viable experimental solution. Acting as physical realizations of the actuator disk model, porous disks extract momentum from the flow and reproduce the dominant wake features of horizontal-axis wind

turbines. Although some blade-resolved effects are not captured, turbulent diffusion progressively attenuates these differences downstream, allowing porous disks to reproduce self-similar velocity profiles in the mid to far wake [2]. This makes them well suited for experimental studies of wake interactions in floating wind farms.

The challenge, however, lies in the physical realization of porous disks. In all the studies, disk design is based on matching the thrust coefficient of the reference turbine, which ensures global momentum equivalence but does not uniquely define the disk properties. Consequently, a wide variety of porous disk designs have been reported in the literature [3–6], often producing different wake characteristics.

2. Objectives

The objective of this work is to develop and assess an optimized design for porous disks capable of reproducing the wake characteristics of floating offshore wind turbine rotors under both static and imposed-motion conditions. The proposed approach leverages a Darcy–Forchheimer porous media formulation within a computational fluid dynamics (CFD) framework [7], in which the resistance coefficients are directly linked to the local solidity distribution of the disk. This formulation enables a direct correspondence between numerical model parameters and physically realizable disk designs. Building on previous applications to bottom-fixed turbines - where accurate wake deficit predictions were achieved even under yawed conditions [8] - the porous media approach is here extended to floating configurations, including imposed surge and pitch motions. Three porous disk designs with different radial solidity distributions are considered, all constrained to match the thrust coefficient of a reference three-bladed rotor. The solidity distributions are first calibrated using experimental wake measurements obtained under static conditions, and subsequently assessed under imposed motion cases representative of floating wind turbine dynamics. Beyond validation, the porous media CFD framework is exploited as a design tool for guiding the physical realization of porous disks to be used in future experimental campaigns.

The remainder of the paper is organized as follows. Section 3 describes the disk design strategies, while Section 4 presents the wind tunnel experiments and the CFD setup. Section 5 provides hints on how to switch from the numerical study to the physical realizations of the disk. The main results, covering both static and imposed motion cases and highlighting the differences between the disk prototypes, are presented in Section 6. Finally, conclusions are drawn in Section 7.

3. Disk design strategy

A unique design methodology for porous disks for wind turbine wake modelling is currently missing [4, 9]. Imposing equivalence between the disk drag and the rotor thrust as a design criterion does not uniquely define the radial distribution of disk porosity. Consequently, different disk realizations can produce the same global thrust while generating different wake properties, especially in the mid-wake region [4]. To address this limitation, the present study considers three distinct disk designs, each characterized by a different radial solidity distribution but all constrained to match the thrust coefficient of the reference three-bladed rotor.

3.1. Disk A: uniform porosity disk

The first design consists of a porous disk with a uniform porosity distribution over the entire disk area. In this case, the resistance coefficients in the Darcy–Forchheimer model are spatially constant, resulting in a homogeneous momentum deficit across the disk. This configuration

represents the simplest realization and serves as a baseline for comparison, as it is frequently adopted in actuator disk modelling due to its straightforward implementation.

3.2. Disk B: Blade-lift-inspired porosity distribution

The second design features a radially varying porosity distribution derived from the normal force distribution along the blades of the model wind turbine. The rationale is that the local aerodynamic loading of the rotor blades governs the spatial distribution of momentum extraction from the flow. By mapping the blade lift distribution onto an equivalent disk solidity distribution, this design aims to more accurately reproduce the radial variation of induced velocity and, consequently, the mid- and far-wake characteristics of the rotor. The resulting disk exhibits higher solidity in regions corresponding to higher blade loading and lower solidity toward the root and tip regions, while maintaining the same integrated thrust as the reference rotor. Blade normal force density has been obtained with OpenFAST and the result is shown in Figure 1. Density is discretized in 3 different regions, that will correspond to mid-, high- and low-resistance areas respectively in the disk.

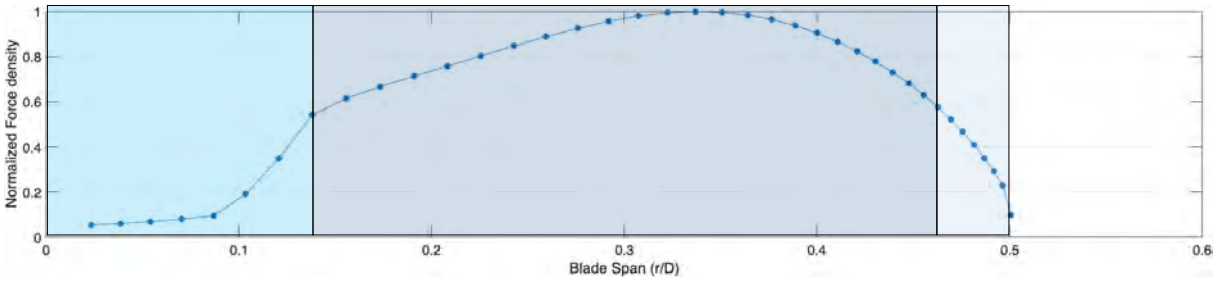

Figure 1. Normalized normal force distribution.

3.3. Disk C: Literature-inspired porosity distribution

The third design is based on solidity distributions reported in [3, 4], where empirical or semi-empirical radial variations are introduced to better approximate measured wake profiles. Specifically, the rationale is to mimic the solidity of the rotor, with highest value in the hub region and decreasing when radially moving to the tip region.

3.4. Validation procedure

The performance of the three disk designs is first evaluated under static conditions by comparing the resulting wake velocity deficits at different distances downstream against experimental measurements obtained for the three-bladed rotor. The disk design that provides the closest agreement in static conditions is then further assessed under imposed motion cases representative of floating wind turbine dynamics.

4. Experimental and numerical setups

4.1. Wind tunnel tests

Experimental data are gathered in a campaign at the Open Jet Facility of Delft University of Technology. The tests involve a 1:148 scale model of the DTU 10 MW reference wind turbine, mounted on a six degrees-of-freedom parallel kinematic robotic platform. The model has a rotor diameter of $D = 1.2\,\mathrm{m}$, a hub height of $H = 0.8\,\mathrm{m}$, and a thrust coefficient $C_T = 0.79$. Further details about the hybrid setup are provided in [10]. The wake flow is measured with particle

tracking velocimetry technique using helium-filled soap bubbles, acquiring images with four high-speed cameras and illuminating the particles with two LEDs. Monitored volumes span from 1D to 5D, as clarified in Figure 2, allowing the characterization of the near- and mid-wake. Tests are performed with an inlet wind speed $U_{ref} = 4\,\mathrm{m/s}$ and turbulence intensity $I_U^y = 2\%$. The motion cases are sinusoidal displacements in surge and pitch direction with reduced frequencies of $St = 0.6$ and a normalised velocity variation amplitude of $\Delta V/U = 0.1$. Reduced frequency of 0.6 is selected to match the pitch natural frequency for a 10MW floating turbine and used for both pitch and surge cases to highlight any difference due to the motion type.

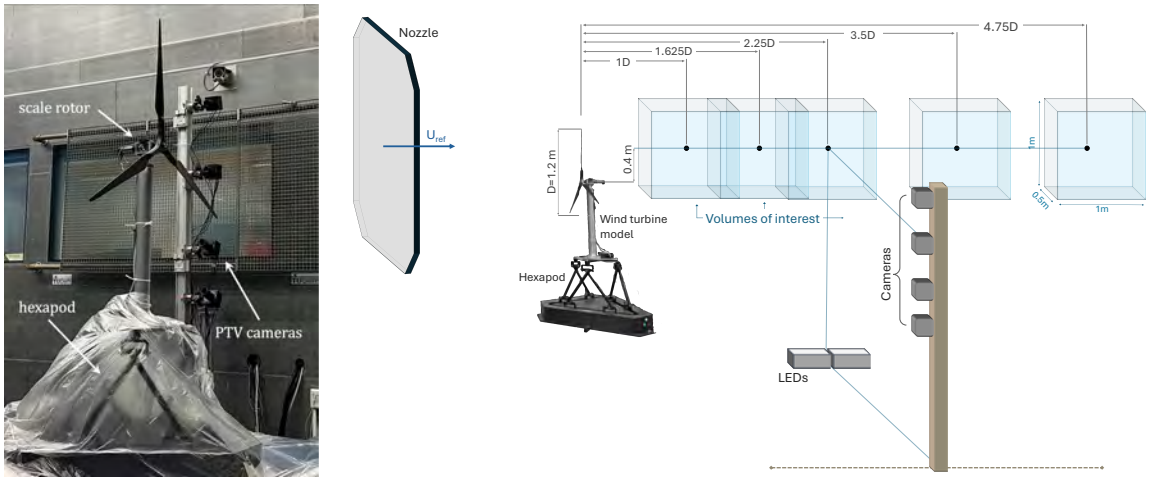

Figure 2. Experimental setup picture (left) and sketch (right).

4.2. CFD model

The porous disk is modelled within a CFD framework using a Darcy–Forchheimer (D-F) approach to represent the momentum losses induced by the disk. This formulation allows to represent the disk through a set of cells where a sink term is added to the momentum balance equation [7]. In this way, the disk can be characterized through resistance coefficients, eventually radially varying, which are directly related to the local porosity of the disk. According to the Darcy-Forchheimer law, already used in wind energy applications by [8], the sink term is defined as:

$$\mathbf{s} = -\frac{1}{2}\rho U \mathbf{F}\mathbf{u}\,, \tag{1}$$

where $\mathbf{u} = [u_x, u_y, u_z]'$ is a vector of the fluid velocity components, $U = \|\mathbf{u}\|$, ρ the air density, and $\mathbf{F}$ is the Forchheimer tensor, represented through a diagonal matrix.

Assuming an incompressible steady-state flow, the momentum balance equation at the root of the CFD model becomes:

$$\frac{\partial u_j u_i}{\partial x_j} = \frac{\partial}{\partial x_j}\left(\mu \frac{\partial u_i}{\partial x_i}\right) + \frac{1}{\rho}\frac{\partial p}{\partial x_i} - \frac{1}{2} U f_i u_i \quad \text{with } i,j = x,y,z\,, \tag{2}$$

where p is the fluid pressure, f_i are the terms of $\mathbf{F} = \mathrm{diag}(f_x, f_y, f_z)$, and they represent the resistance of the disk.

4.2.1. Choice of the resistance coefficients. The coefficient f_x, which characterizes the resistance term when the flow is normal to the disk, is differentiated between different disk designs to represent different solidity distribution. Firstly, for disk A, the coefficient is chosen such that the drag force of the disk matches with the wind turbine thrust. For disk B, the coefficient is

differentiated between the inner region and the outer one, while three different annular regions are identified for disk C with resistance coefficient decreasing moving from the hub in radial direction. Since all the disks are tested just in conditions normal to the flow (no yawed conditions), resistance terms in directions y and z are set equal to zero, since they are expected to play no role in wake generation for static and surge cases. For the pitch amplitudes and reduced frequencies considered in this study, the induced transverse velocity components are expected to remain small compared to the streamwise velocity. For this reason, the tensor is kept diagonal with one non-null coefficient even for the pitch case. Figure 3 summarizes the selected parameters for the three designs, with $f_x = f/h$, where h is the thickness of the porous region in the computational domain.

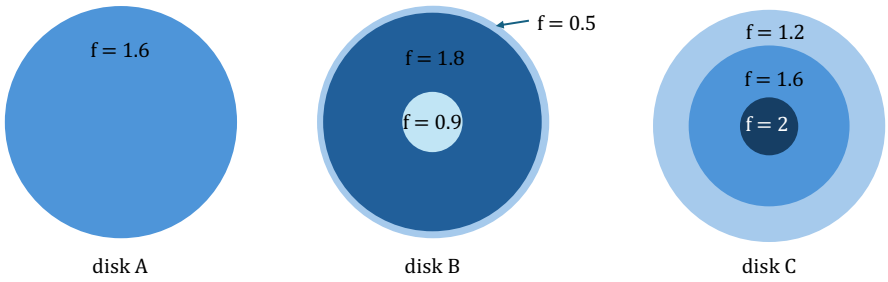

Figure 3. Disk solidity distributions tested: the f parameter is the input in the D-F model.

4.2.2. Numerical Setup. The computational domain mimics the experimental environment, as depicted in Fig. 4. The domain is symmetric with respect to the vertical plane passing through the disk and has wall-boundary conditions to represent the wind tunnel walls. The region of the wind tunnel occupied by the bladed rotor is replaced in the simulation by a porous volume. The thickness of the porous volume is $h = 0.3$ m; the mesh has been refined in correspondence of the porous volume to have at least 5 cells in the x direction. This is required to properly realize the momentum deficit $\mathbf{s}$ of Eq. 1. Simulations have been repeated, changing the porous region thickness, proving that results are independent from this parameter.

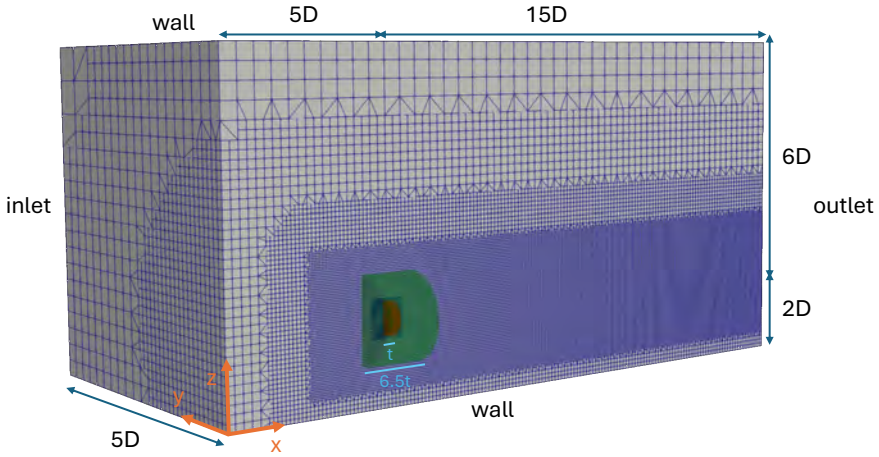

Figure 4. CFD domain and setup.

The numerical simulations are performed using OpenFOAM with RANS and URANS solvers

for the static and imposed motion cases respectively, with a second-order differentiation scheme. The $k-\omega$ shear stress transport (SST) model has been used. The computational domain is meshed with 1.5 million hexahedral elements and five refinement levels. The independence of the results on the mesh refinement has been checked and is not reported here for brevity. All the motions experimentally tested are reproduced in the numerical model, assigning prescribed sinusoidal motion on a designated cell zone around the disk (green zone in Figure 4).

5. Indications on the physical realisation of the disk

After defining the solidity distributions (Section 3) and their implementation through the Darcy–Forchheimer resistance coefficients within the CFD framework (Section 4), the present section illustrates how these numerical designs can be translated into physically manufacturable porous disks. The main advantage of relying on the D–F porous media model to represent the wake of a bladed rotor is the possibility of obtaining guidance on the physical realization of porous disks for experimental investigations. In particular, the model enables a direct link between the numerically prescribed resistance coefficients and the geometrical properties of the disk, mainly its porosity distribution.

As an example of possible physical realizations based on the design methodology proposed in this study, Figure 5 shows three porous disk configurations. Following the drag–porosity relationship proposed by [9], the ratio of void area to total disk area is first set to 55% in order to match the thrust of the reference wind turbine. This single constraint is used to define the uniform disk design A. For disks B and C, the disk area is discretized according to the radial solidity distributions investigated in the CFD simulations. Each region is then assigned a local void-to-total area ratio based on the corresponding resistance coefficients, while enforcing that the overall disk porosity remains equal to 55% to ensure the same total drag.

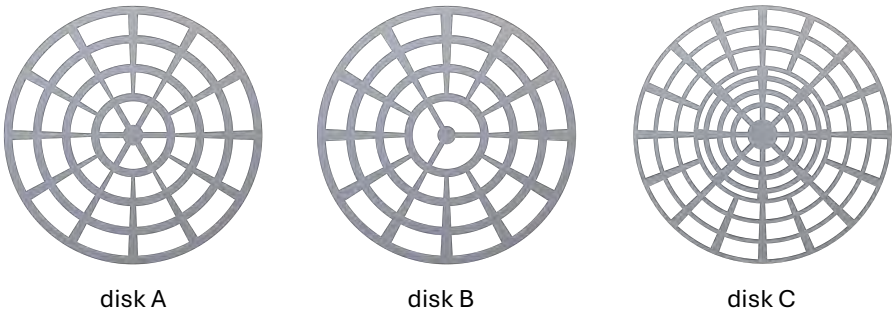

Figure 5. Disks realisation based on the resistance coefficients distribution from Darcy-Forchheimer model.

6. Results

6.1. Static Case

Figure 6 compares the normalized wake velocity fields obtained from CFD simulations for disks A, B, and C, with data extracted on the mid-plane x–z. Differences among the disk designs are most pronounced in the near- to mid-wake region, i.e. between $1.5D$ and $4D$, where the velocity distributions reflect the imposed solidity distributions. Although a porous disk cannot

reproduce blade-induced swirl or coherent tip vortices expected in the immediate near wake, the comparison at $x/D \approx 1$–1.5 is retained to assess the direct influence of the prescribed solidity distribution on the mean velocity deficit immediately downstream of the disk. The objective in this region is not to replicate blade-resolved flow structures, but to evaluate how the radial resistance distribution shapes the initial wake profile before turbulent mixing progressively reduces these differences further downstream. Disk A shows an approximately uniform velocity deficit across the disk area, consistent with its uniform solidity distribution. Disk B incorporates a reduced resistance coefficient in the hub region, resulting in locally higher velocities near the center compared to the surrounding disk area. In contrast, disk C displays a velocity deficit that decreases radially from the hub toward the outer region, leading to increasing velocity with radial distance. Further downstream ($x/D > 4$), the differences between the disk designs progressively diminish, indicating a reduced sensitivity of the wake to the disk solidity distribution. This behavior is consistent with experimental observations reported by [4].

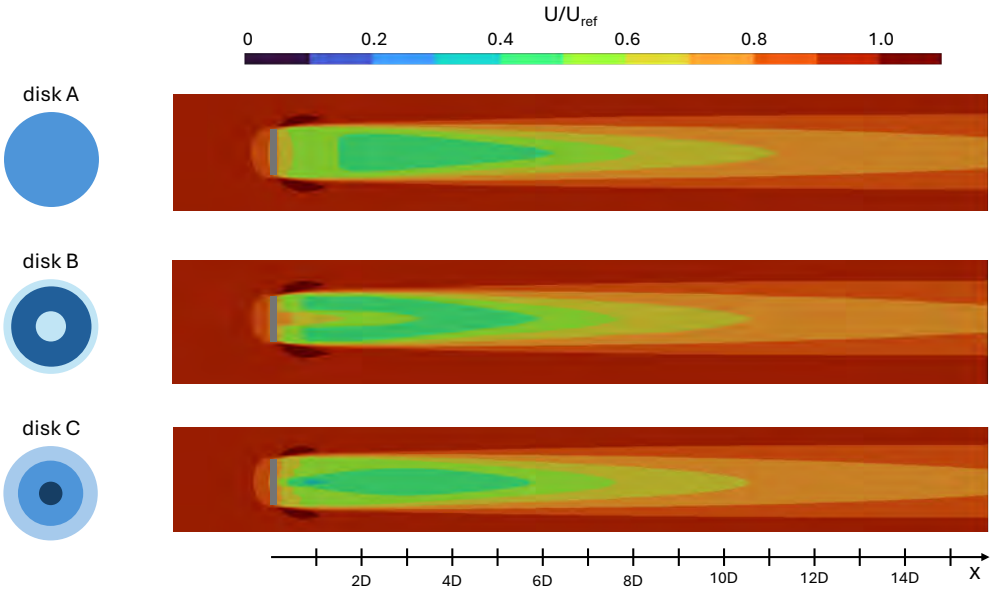

Figure 6. Normalized wake deficit from CFD simulations for different disk designs.

For a more quantitative comparison, vertical velocity profiles are extracted at selected downstream locations and shown in Figure 7, together with the corresponding experimental data. The profiles refer to the upper half of the rotor, as this is the region where experimental measurements are available. The z-coordinate is oriented upward and centered at the hub height. At $x/D = 1.5$, none of the disk configurations fully captures the experimental velocity deficit. Among the three designs, disk B provides the closest agreement, reproducing the characteristic S-shaped profile observed in the experiments, with a good match of the deficit in the hub region and an underestimation toward the tip. An opposite trend is observed for disk C, which exhibits a radial variation of the deficit that contrasts with that of the bladed rotor. The uniform disk (A) instead yields an almost flat velocity profile across the rotor region. Moving downstream, disk A maintains a self-similar velocity profile and shows improved agreement with the experimental data from $x/D = 4.5$ onward. Conversely, the initially S-shaped profile of disk B progressively becomes more uniform, achieving an almost perfect match with the experimental data at $x/D = 3$. Beyond $x/D = 4.5$, the velocity profiles of all disk designs collapse onto a

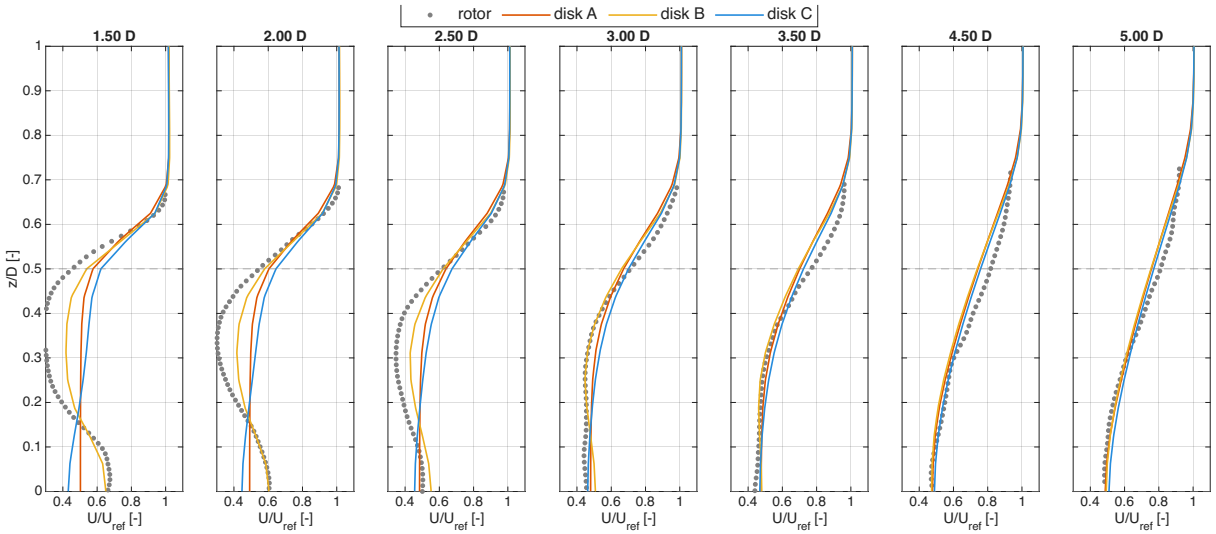

Figure 7. Normalized wind speed in the disk wake extracted in the vertical plane from hub to tip region, at distances from 1.5D to 5D for different disk designs and 3-bladed rotor.

single curve, which presents the Gaussian-like shape, showing very good agreement with the wake measured behind the bladed rotor.

Despite similarities between disks in the mid- to far-wake region, disk B is the one that best approximates the rotor behaviour, even for shorter distances. For this reason, in the following, results from imposed motion cases are limited to this disk.

6.2. Imposed motions

6.2.1. Surge case. For the imposed surge motion at $St = 0.6$, time-averaged normalized streamwise velocity profiles (U/U_{ref}) are extracted on the mid-plane ($y = 0$) at different downstream locations and compared with the experimental data obtained from the bladed rotor. Results are shown in Figure 8, where experimental data from the static case are also included for reference. Even under imposed motion, the near-wake characteristics are influenced by the distribution of the disk resistance coefficients, resulting in non-uniform velocity profiles at $x/D = 1.5$ and 2. At these locations, the porous disk sligthly underestimates the wake deficit in the region $0.15 < z/D < 0.5$ when compared to the experimental data. Further downstream, the velocity profiles obtained under imposed motion progressively converge, showing very good agreement with the experimental data at $x/D = 3$. At larger downstream distances, the experimental wake profiles depart from the static case, indicating a faster wake recovery under imposed surge motion. While the porous disk reproduces this trend, it predicts a slower wake recovery than that observed experimentally for the bladed rotor.

6.2.2. Pitch case Figure 9 shows the mean vertical velocity profiles extracted on the mid-plane ($y = 0$) at different downstream locations and compared with the experimental data obtained from the bladed rotor. Experimental results indicate that, in the near-wake region, the velocity profiles exhibit a non-uniform distribution within the rotor area, with the strongest velocity deficit occurring at $z/D \approx 0.35$. The porous disk reproduces the same qualitative trend, although the magnitude of the velocity deficit is underestimated. From $x/D = 2.5$ onward, the numerical and experimental profiles predict a similar mean wake behavior, and a good level of consistency between the two approaches is maintained for all the analyzed downstream locations. Finally, it is to noting that the CFD simulations show only minor differences between surge and pitch

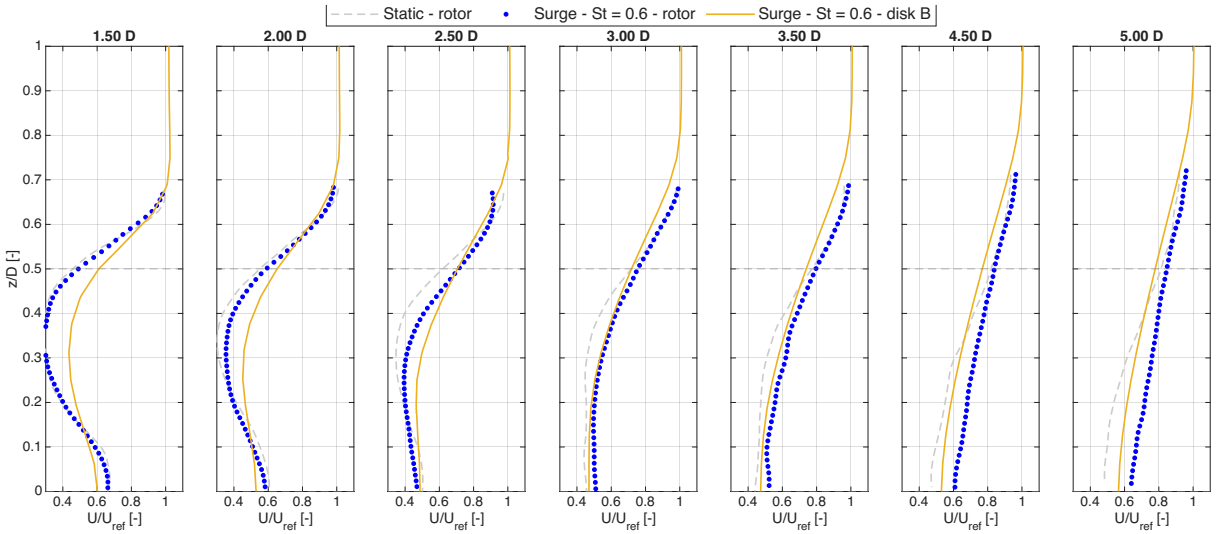

Figure 8. Normalized mean wind speed in the wake extracted from the vertical plane from hub to tip region, at distances from 1.5D to 5D for different disk designs and bladed rotor in surge motion.

motions in terms of wake behavior. Experimental measurements, however, suggest that surge motion is more effective than pitch motion in promoting wake recovery. This discrepancy could be due to different turbulent wake structures that seem not to be caught by the CFD model.

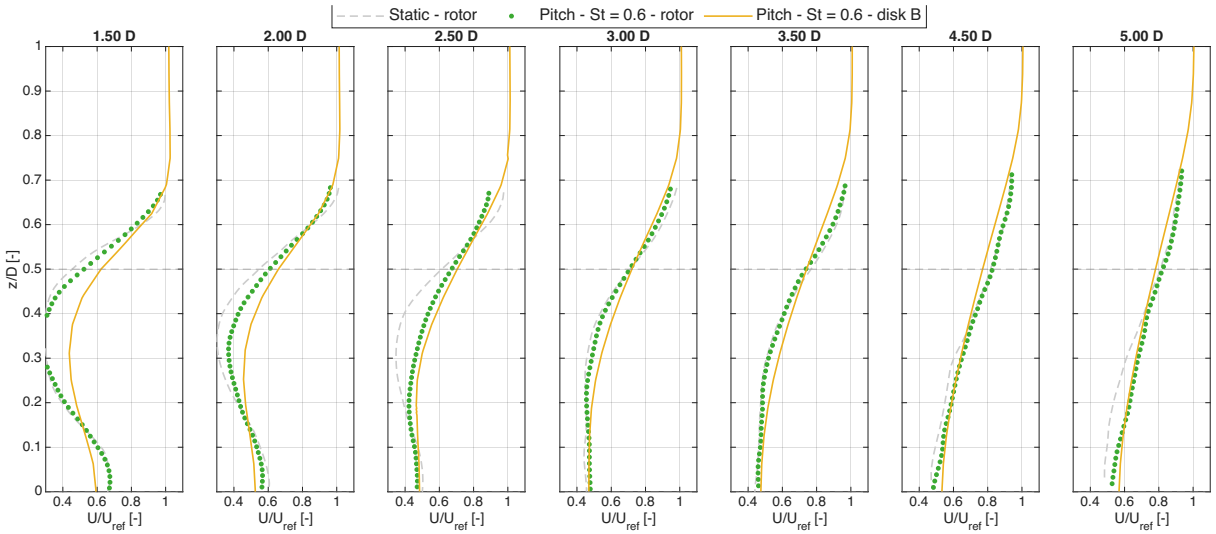

Figure 9. Normalized mean wind speed in the wake extracted from the vertical plane from hub to tip region, at distances from 1.5D to 5D for different disk designs and 3-bladed rotor in pitch motion.

7. Conclusions

This work proposed and assessed a rational design methodology for porous disks aimed at reproducing the wake characteristics of floating offshore wind turbine rotors under both static and imposed-motion conditions. The approach combines a Darcy–Forchheimer porous media formulation within a CFD framework with systematic variations of the disk solidity distribu-

tion, enabling a direct link between numerical model parameters and physically realizable disk designs. Three porous disk configurations with different radial solidity distributions were investigated, all constrained to match the thrust coefficient of a reference three-bladed rotor. Under static conditions, the disk solidity distribution was shown to strongly influence the near- and mid-wake structure, while its effect diminished downstream. In particular, the disk with a non-uniform solidity distribution based on the blade normal force provided the closest agreement with experimental velocity deficits in the mid-wake region. Beyond $4D$, the wake profiles of all disk designs collapsed and exhibited very good agreement with the experimental data. Under imposed platform motions, the porous disk model captured the main experimental trends, including changes in wake recovery associated with surge and pitch motion. While differences between disk designs persisted in the near wake, the wake response became progressively less sensitive to the solidity distribution downstream. Compared to the bladed rotor, the porous disk reproduced the wake dynamics qualitatively but with a slightly slower recovery for surge case. Comparison proved good even quantitatively for the pitch case instead. By relating resistance coefficients to disk porosity, the proposed methodology provides practical guidance for the physical realization of porous disks. Overall, the approach can provide support in designing hybrid experimental–numerical investigations of scaled floating wind farms, enabling more systematic and reproducible studies of wake interactions under unsteady platform dynamics.

Finally, to further improve the representativeness of the porous disk approach for floating wind turbine applications, disk design should also account for load variations. In particular, future research should evaluate the evolution of aerodynamic loads and compare them with those expected from a bladed rotor. Thrust variations induced by platform motion may depend on the radial solidity distribution of the disk. Assessing whether porous disk realizations can reproduce these load dynamics consistently with bladed rotors represents an important step toward extending the present methodology to floating farm studies.

Acknowledgements

The authors would like to acknowledge the international mobility program of the Mechanical Engineering Department of Politecnico di Milano and the IDEA League fellowship for the financial support given to carry on this work.

References

[1] Soares-Ramos E P, de Oliveira-Assis L, Sarrias-Mena R and Fernández-Ramírez L M 2020 Current status and future trends of offshore wind power in Europe *Energy* **202** 117787 URL https://doi.org/10.1016/j.energy.2020.117787

[2] Camp E H and Cal R B 2016 Mean kinetic energy transport and event classification in a model wind turbine array versus an array of porous disks: Energy budget and octant analysis *Phys. Rev. Fluids* **1**(4) 044404 URL https://doi.org/10.1103/PhysRevFluids.1.044404

[3] Bourhis M and Buxton O 2024 Influence of freestream turbulence and porosity on porous disk-generated wakes *Physical Review Fluids* **9** 124501 URL https://doi.org/10.1103/PhysRevFluids.9.124501

[4] Kurelek J W, Piqué A and Hultmark M 2023 Performance of the porous disk wind turbine model at a high Reynolds number: Solidity distribution and length scales effects *Journal of Wind Engineering and Industrial Aerodynamics* **237** 105377 URL https://doi.org/10.1016/j.jweia.2023.105377

[5] Wosnik M *et al.* 2020 Wake meandering in a model wind turbine array in a high reynolds number turbulent boundary layer *Journal of Physics: Conference Series* vol 1452 (IOP Publishing) p 012073 URL https://doi.org/10.1088/1742-6596/1452/1/012073

[6] Aubrun S, Loyer S, Hancock P E and Hayden P 2013 Wind turbine wake properties: Comparison between a non-rotating simplified wind turbine model and a rotating model *Journal of Wind Engineering and Industrial Aerodynamics* **120** 1–8 URL https://doi.org/10.1016/j.jweia.2013.06.007

[7] Marykovskiy Y, Pomaranzi G, Schito P and Zasso A 2024 A method to evaluate Forchheimer resistance coefficients for permeable screens and air louvers modelled as a porous medium *Fluids* **9** 147 URL https://doi.org/10.3390/fluids9070147

[8] Catania M, Pomaranzi G, Fontanella A and Zasso A 2024 Modelling of wind turbines as porous disks for wind farm flow studies *Journal of Physics: Conference Series* **2767** URL https://doi.org/10.1088/1742-6596/2767/5/052049

[9] Lignarolo L E, Ragni D, Ferreira C J and van Bussel G J 2016 Experimental comparison of a wind-turbine and of an actuator-disc near wake *Journal of Renewable and Sustainable Energy* **8** URL https://doi.org/10.1063/1.4941926

[10] Taruffi F, Novais F and Viré A 2024 An experimental study on the aerodynamic loads of a floating offshore wind turbine under imposed motions *Wind Energy Science* **9** 343–358 URL https://doi.org/10.5194/wes-9-343-2024